

# Scent of the familiar: An fMRI study of canine brain responses to familiar and unfamiliar human and dog odors



Gregory S. Berns<sup>a,\*</sup>, Andrew M. Brooks<sup>a</sup>, Mark Spivak<sup>b</sup>

<sup>a</sup> Center for Neuropolicy, Emory University, Atlanta, GA 30322, United States

<sup>b</sup> Comprehensive Pet Therapy, 6600 Roswell Road, Suite K-2, Sandy Springs, GA 30328, United States

## ARTICLE INFO

### Article history:

Available online 6 March 2014

### Keywords:

fMRI  
Canine  
Olfaction  
Social cognition  
Reward

## ABSTRACT

Understanding dogs' perceptual experience of both conspecifics and humans is important to understand how dogs evolved and the nature of their relationships with humans and other dogs. Olfaction is believed to be dogs' most powerful and perhaps important sense and an obvious place to begin for the study of social cognition of conspecifics and humans. We used fMRI in a cohort of dogs ( $N = 12$ ) that had been trained to remain motionless while unsedated and unrestrained in the MRI. By presenting scents from humans and conspecifics, we aimed to identify the dimensions of dogs' responses to salient biological odors – whether they are based on species (dog or human), familiarity, or a specific combination of factors. We focused our analysis on the dog's caudate nucleus because of its well-known association with positive expectations and because of its clearly defined anatomical location. We hypothesized that if dogs' primary association to reward, whether it is based on food or social bonds, is to humans, then the human scents would activate the caudate more than the conspecific scents. Conversely, if the smell of conspecifics activated the caudate more than the smell of humans, dogs' association to reward would be stronger to their fellow canines. Five scents were presented (self, familiar human, strange human, familiar dog, strange dog). While the olfactory bulb/peduncle was activated to a similar degree by all the scents, the caudate was activated maximally to the familiar human. Importantly, the scent of the familiar human was not the handler, meaning that the caudate response differentiated the scent in the absence of the person being present. The caudate activation suggested that not only did the dogs discriminate that scent from the others, they had a positive association with it. This speaks to the power of the dog's sense of smell, and it provides important clues about the importance of humans in dogs' lives.

This article is part of a Special Issue entitled: Canine Behavior.

© 2014 The Authors. Published by Elsevier B.V. This is an open access article under the CC BY-NC-ND license (<http://creativecommons.org/licenses/by-nc-nd/3.0/>).

## 1. Introduction

Dogs' perceptual experience of their environment remains inscrutable. But understanding dogs' perceptual experience of both conspecifics and humans is important to understand how dogs evolved and why humans find them so appealing. Because we can only intuit their perceptions from their behaviors, traditional methods may fail to elucidate what dogs actually perceive and whether they have emotional responses similar to humans (Darwin, 1872; Panksepp, 2004; Bekoff, 2007). A resurgence in canine behavioral science is revealing the extent of dogs' cognitive skills (Hare and Woods, 2013; Miklosi, 2007), but critical questions about their

social intelligence remain unanswered. Recent evidence, for example, suggests that dogs form strong attachments to humans (Topal et al., 1998; Palmer and Custance, 2008; Miklosi and Topal, 2013), and that these attachments may be stronger than to conspecifics. However, we do not know whether this behavior is primarily a result of heredity or the environment in which dogs are raised (Udell and Wynne, 2010; Udell et al., 2010).

Olfaction is believed to be dogs' most powerful and perhaps important sense and an obvious place to begin for the study of social cognition of conspecifics and humans (Thesen et al., 1993; Miklosi, 2007). Anecdotal evidence suggests that dogs can discriminate conspecifics by odor (Bekoff, 2001), and well-trained dogs can match scents from different parts of the body of the same person as well as twins (Hepper, 1988; Schoon and de Bruin, 1994). But these skills are behavioral manifestations of internal mental states and do not tell us directly what dogs think about either humans or other dogs.

\* Corresponding author. Tel.: +1 404 727 2556.  
E-mail address: [gberns@emory.edu](mailto:gberns@emory.edu) (G.S. Berns).

Here, we used fMRI in a cohort of dogs ( $N = 12$ ) that had been trained to remain motionless while unsedated and unrestrained in the MRI (Berns et al., 2012, 2013). By presenting scents from humans and conspecifics, we aimed to identify the salient dimensions of dogs' social cognition – whether it is based on species (dog or human) or familiarity. During fMRI, dogs were presented with five scents: (1) self; (2) familiar human; (3) strange human; (4) familiar dog; (5) strange dog.

A vast literature on the caudate in humans, monkeys, and rats points to this region's role in positive expectations (Montague and Berns, 2002; Schultz et al., 1997; Knutson et al., 2001), including social rewards (Rilling et al., 2002; Izuma et al., 2008). Anatomically, the caudate receives widespread inputs from the cortex in the form of glutamatergic (excitatory) neurons and modulatory inputs from the dopaminergic neurons in the brainstem (Koob, 1992). The output of the caudate goes to globus pallidus and the thalamus, which form multiple parallel loops back to the cortex (Alexander et al., 1986). Computational models suggest that dopamine release in the caudate acts as a signal of “reward prediction error” (Schultz et al., 1997), meaning that rewarding stimuli that are unexpected or increase an animal's expectation for reward, are associated with both dopamine release in the caudate and the hemodynamic response as measured with fMRI. Within this framework, caudate activity is correlated with salient, usually rewarding, signals that cause the animal to change its behavioral orientation to approach or consume the stimulus (Daw et al., 2011).

Because of these well-known association with positive expectations (Berridge and Robinson, 2003; Knutson et al., 2001; Montague and Berns, 2002; Schultz et al., 1997), and because of its clearly defined anatomical location, we focused our analysis on the dog's caudate nucleus. We hypothesized that if dogs' primary association to reward, whether it is based on food or social bonds, is to humans, then the human scents would activate the caudate more than the conspecific scents. Conversely, if the smell of conspecifics activated the caudate more than the smell of humans, dogs' association to reward would be stronger to their fellow canines.

## 2. Material and methods

### 2.1. Participants

This study was performed in strict accordance with the recommendations in the Guide for the Care and Use of Laboratory Animals of the National Institutes of Health. The study was approved by the Emory University IACUC (Protocol # DAR-2001274-120814BA). All dogs' owners gave written consent for participation in the study. All dogs (Table 1 and Fig. 1) had previously completed an fMRI session in which two hand signals were given, one indicating the imminent receipt of a food reward, and the other indicating no reward (Berns et al., 2012, 2013). Thus, all dogs had demonstrated their ability to remain motionless during fMRI for periods up to 30 s and consistently during the interval between hand signal and reward.

### 2.2. Training

Based on our initial experience, we developed a training program for the dogs that teaches them to cooperatively enter the MRI scanner (Berns et al., 2013). The program was based on acclimatization to the MRI scanner noise, tight scanner enclosure, scanner steps, and operating vibrations and the shaping and ultimate chaining of several requisite behaviors. To do this, we constructed two replica MRIs, each of which consisted of a tube of approximately the same dimensions as the inner bore of the actual Siemens MRI, a patient table, portable steps, and multiple simulated receiver coils that adhered closely to the dimensions of a human neck coil. We

also constructed a proprietary chin rest that facilitated comfort and proper positioning for the animals and that adapted the apparatus for the uniqueness of the canine anatomy. Once the animals became confident and competent regarding all the preparatory steps – proven by completing a simulated MRI in the replica apparatus – we then performed live scans in the actual MRI.

Because all of the dogs in this experiment had completed a previous MRI scan, no further acclimatization to the MRI environment was necessary. They were all highly proficient remaining in the chin rest, wearing ear muffs, while hearing the scanner sounds. The sound pressure level of the functional sequences had previously been measured at 95 dB. Although it is impossible to know the exact level of noise reduction provided by the ear muffs, the manufacturer estimates a reduction of 25–28 dB when properly fitted ([www.safeandsoundpets.com](http://www.safeandsoundpets.com)). Even if the muffs provided only a 10 dB reduction in noise, that would bring the ambient sound pressure level down to 85 dB, which is considered safe for a human for up to 8 h continuously. The dogs' actual exposure time to the MRI noise was less than 30 min.

Training for the smell experiment consisted of biweekly instruction at our training facility and practice at home with the mock head coil and chin rest. Because the dogs were already proficient in the basic behavior of placing the head in the chin rest and remaining motionless, the added training was aimed at acclimating the dogs to the presentation of a cotton swab in front of the nose. Using 6-in. sterile cotton swabs, handlers moved the swab to within a centimeter of the dog's nose. In the initial stage of training, dogs were rewarded quickly for not moving either toward or away from the swab. This was achieved through either clicker or praise and followed by a food reward. Once dogs demonstrated proficiency at not reacting to the swab, we replaced the clicker and praise with the hand signal learned in the original experiment. The hand signal thus functioned as a “visual clicker” indicating correct behavior and imminent reward (because clickers cannot be heard reliably in the scanner). The swab was presented for approximately 3 s, with at least 10 s between presentations. The number of swab presentations between rewards was gradually increased from 0 to 6 (the maximum that would occur in the actual MRI experiment), and ultimately was random. The total time in training, which was calculated as the number of days between the original MRI experiment and the smell MRI, was 67 days (range: 26–113 days).

### 2.3. MRI scanning

All scanning was performed on a Siemens 3 T Trio whole-body scanner. Instead of the birdcage head coil used in our previous study, we found that using a standard neck coil placed the active element closer to the dog's brain (Berns et al., 2013). Although less homogeneous in coverage than the birdcage, the upper element was in close proximity to the dog's brain, which provided a superior signal-to-noise ratio (SNR) of the brain in comparison to the birdcage coil, especially at the dorsal part of the brain (SNR ~40 vs. 17 with birdcage.) More importantly, because the dog's shoulders and body were outside of the coil, we were less constrained by subject size. We could accommodate larger heads by simply lowering the chin rest. Two dogs (McKenzie and Huxley) used the birdcage coil before we switched to the neck coil in the other dogs. As an attempt to measure sniffing, five of the dogs also wore the Siemens wireless respirometer, which is a small air-filled bladder that was held in place with a Thundershirt®. Due to the small number of subjects and the inconsistency of the data obtained, the respiratory data were not used in the analysis.

First, a single sagittal plane image was acquired as a localizer, which lasted 3 s (SPGR sequence, slice thickness = 4 mm, TR = 9.2 ms, TE = 4.16 ms, flip angle = 40°, 256 × 256 matrix, FOV = 220 mm). The localizer sound tended to be the most startling

**Table 1**  
Demographics of dogs.

Dog	Breed	Sex	Age (yrs)	Weight (lbs)	Service or therapy dog training?
Zen	Yellow Lab	Male – neutered	3	70	Y
Tigger	Boston Terrier	Male – neutered	6	26	Y
Pearl	Golden Retriever	Female – spayed	3	50	Y
McKenzie	Border Collie	Female – spayed	4	35	N
Kady	Yellow Lab	Female – spayed	2	52	Y
Eli	Viszla	Male – intact	4	60	N
Caylin	Border Collie	Female – spayed	4	44	N
Callie	Feist	Female – spayed	3	25	N
Myrtle	Black Lab	Female – spayed	7	55	Y
Huxley	Lab mix	Male – neutered	2	40	N
Libby	Pit mix	Female – spayed	7	50	N
Stella	Bouvier	Female – spayed	5	65	N

and unpleasant for the dogs. This was minimized by acquiring a single plane. For functional scans, we used single-shot echo-planar imaging (EPI) to acquire volumes of 24 sequential 3 mm slices with a 10% gap (TE = 28 ms, TR = 1400 ms, flip angle = 70°, 64 × 64 matrix, 3 mm in-plane voxel size, FOV = 192 mm). Slices were oriented dorsally to the dog's brain (coronal to the magnet because the dog was positioned 90° from the usual human orientation) with the phase-encoding direction right-to-left. Sequential scans were

preferred to minimize between-plane offsets when the dog moves. The 10% slice gap minimized crosstalk for sequential acquisitions. For each dog, two runs up to 600 volumes were acquired, each lasting about 7–14 min. After the functional runs, a T2-weighted structural image was acquired with a turbo spin-echo sequence (25 2 mm slices, TR = 3940 ms, TE = 8.9 ms, flip angle = 131°, 26 echo trains, 128 × 128 matrix, FOV = 192 mm), which lasted 24 s.



**Fig. 1.** Dog participants. The 12 dog participants resting, training, and wearing Mutt Muffs. Of particular note, the photo of Kady demonstrates a training repetition using a mock receiver coil, chin rest, and cotton-tipped applicator presentation that duplicates the protocol incorporated in the MRI scan.



## 2.4. Stimuli

Scents were collected the morning of the scan on sterile gauze pads and sealed in Mylar envelopes. Human scents were collected from the armpit (sans deodorant), and dog scents were collected from the perineal-genital area. The familiar human was either a member of the dog's household (but not the handler because their scent would be pervasive throughout the MRI scanning) or a close friend. The familiar dog was another dog in the household. Strange scents were collected from individuals whom the dog had never met and were matched for sex to the corresponding familiar scents. Prior to scanning, a strip was cut from each gauze pad and wrapped around the end of a 6-in. cotton-tipped applicator. These were numerically coded. The handler was blind to the code to prevent inadvertent signaling of the identity of the scents.

Within the MRI, the handler presented 10 repetitions of each scent (50 trials), divided into two functional runs. The scent was presented in front of the dog's nose for approximately 3 s, with approximately 10–15 s between trials. The intertrial time was necessary to allow accurate measurement of the hemodynamic response, which peaks at approximately 6 s after the onset of a stimulus. The two functional runs lasted 7–14 min, which depended on the speed of the handler's presentation between successive stimuli. The order of the scents was random but equal in number for each run. In addition to the 5 scents, 9 reward trials were interspersed within each run. Reward trials were of the same form as the previous experiment: a hand signal for 5–10 s, followed by the delivery of a piece of food. The number of scent presentations between reward trials was also random and varied from 0 to 6.

## 2.5. Event recording

Trial events were recorded by an observer via a four-button MRI-compatible button-box. The observer stood next to the handler at the head-end of the MRI and could see the dog in the bore of the magnet. The observer marked these events: scent presentation onset and offset, hand signal onset, and reward. The onset of a scent trial was marked when the swab was in the proximity of the dog's nose. The offset was marked when the handler retracted it. A laptop running Matlab (MathWorks) and Cogent (FIL, University College London) was connected via serial port to the button box, and recorded both the button-box responses by the observer, as well as the scanner sequence pulses. A second assistant, who sat on a stool next to the observer and handler and wore nitrile gloves, gave the numerically coded swabs to the handler in a predetermined randomized order. Reward trials, which were also predetermined, were signaled to the handler by a tap on the hand, after which the handler gave the hand signal for reward, followed by a treat.

## 2.6. Functional data preprocessing and analysis

All functional data was pre-processed using AFNI and its associated functions. DICOM files of the EPI runs were first converted to AFNI BRIK format using the `to3d` command. The EPI runs were then subjected to motion correction using `3dvolreg`'s 6-parameter affine transformation, employing a two pass method, where the first pass results in a crude alignment and the second pass a fine alignment. All volumes were aligned to a reference volume, which was either the first volume of the first run, or a manually chosen volume from the first run based on a visual inspection.

Three separate methods were used to censor volumes with remaining motion artifacts. First, `3dToutcount` was used to output the fraction of outlier voxels for each volume. `3dToutcount` defines outliers as those voxels whose signal intensity deviates from the median absolute deviation of the time series. Volumes with a fraction larger than 0.01 were censored from the statistical

analysis. Second, `1d_tool.py` was used to censor volumes based on the amount of estimated motion outputted from `3dvolreg`. `1d_tool.py` computes the Euclidean norm of the derivative of the rotation and translation parameters outputted from `3dvolreg`. We then used a Euclidean norm cut-off of 1 to generate the censor file. Finally, we visually inspected the resulting time series with the censored volumes from `3dToutcount` and `1d_tool.py`, and censored any volumes that showed obvious artifact. On average, 61% of the total EPI volumes were retained for each subject (ranging from 43% to 85%), which was an improvement from the previous study (average 43%). The majority of the censored volumes followed the consumption of the food reward with occasional movements following the cotton swab presentation, depending on the dog.

The EPI images were then smoothed and normalized to %-signal change. Smoothing was applied using `3dmerge`, with a 6 mm kernel at Full-Width Half-Maximum (FWHM). The size of the smoothing kernel was chosen based on the physical size of the caudate, which was estimated to be approximately 6 mm wide. To convert signal intensity values to %-signal change, `3dcalc` was used to subtract and then divide by the mean EPI image (generated from the `3dTstat` – mean option, with censored volumes excluded). These values were then converted to percentages by multiplying by 100. These resulting scaled EPI images were then inputted into the General Linear Model.

For each subject, a General Linear Model was estimated for each voxel using `3dDeconvolve`. The task-related regressors in this model included, (1) reward consumption, (2) reward hand signal, (3) familiar dog smell, (4) unfamiliar dog smell, (5) familiar human smell, (6) unfamiliar human smell, and (7) self-smell. All seven task-related regressors were impulse functions – that is, their duration was not modeled. All events were convolved with a single gamma-function, which approximates the hemodynamic response function. To control for subject movement, the 6 motion regressors outputted from `3dvolreg` were also included in the model. To account for differences between runs, a constant and linear drift term was included for each run. Two dogs (Callie and McKenzie) were also presented with the scents of a human acquaintance and a dog acquaintance (both of whom they had met only briefly). These conditions were modeled as separate conditions for these two dogs but not considered further in the group analysis. The acquaintance conditions were not used in any other dogs because it was not feasible to collect these scents in all of the dogs.

## 2.7. ROI analysis

Because the heterogeneity in the canine brain shape and size makes group normalization difficult, our primary analysis was based on two ROIs: the olfactory bulb (OLF) and the caudate nucleus (CD) (Fig. 2). The OLF ROI was used as a check that the scents were, in fact, processed. The OLF ROI was placed anatomically and centered at the tip of the olfactory peduncle as visualized on the mean EPI image for each dog (Leigh et al., 2008; Datta et al., 2012). Because the caudate was not distinct in the EPI images, we used a functional ROI for the caudate guided by the results from our first experiment (Berns et al., 2012, 2013). Previously, we found that a hand signal indicating imminent food reward reliably activates the caudate. Because the same hand signal was also used here to randomly reinforce the dog for holding in position, we used it to functionally locate the caudate in a manner that was independent of the effects of interest, namely the scents. For each dog, we located the slices containing the caudate based on the “chevron” appearance of the internal capsule (the dark, inverted “V” on the transverse slice inferior to the genu of the corpus callosum, green arrow, Fig. 2B). We located the area of peak activation to the hand signal anterior to this and cross-checked the location with the dog's activation in the first experiment to make sure it was near the caudate (Fig. 3). We

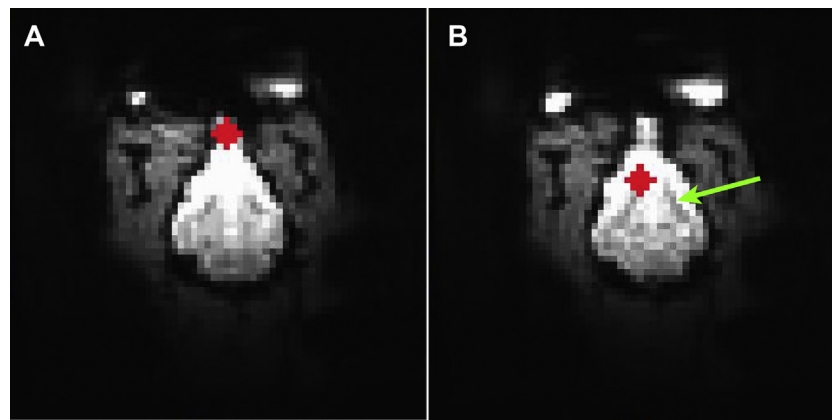


**Fig. 2.** ROI placement. This is an example from Myrtle. The underlay is the mean EPI for two slices showing: (A) olfactory bulb (OLF) placement; and (B) caudate (CD) placement. The internal capsule is identified with the green arrow and served as a landmark for the approximate location of the caudate. The exact location was determined by the voxel in this vicinity with the maximal response to the hand signal indicating reward. ROIs were spheres with 6 mm radius. (For interpretation of the references to color in this figure legend, the reader is referred to the web version of the article.)

then created a spherical ROI with a 6 mm radius centered on the identified cluster of activation.

Average beta coefficients across all voxels in the both the OLF and CD ROIs were calculated for task-related events in the General Linear Model and subsequently analyzed using the Mixed Models procedure in SPSS v21 (IBM). A  $1 \times 5$  ANOVA was formulated with fixed effects for scent (familiar human, strange human, familiar dog, strange dog, self). Dog (i.e. subject) was included as a random effect, and smell as a repeated effect. As an exploratory analysis into the possible sources of heterogeneity between the dogs, we also included a dummy variable in the ANOVA that coded whether the dog was a service-dog. In addition to analyzing the ROIs, we also analyzed the scan-to-scan movement (before motion correction)

using the same ANOVA. The movement was calculated by taking the backward difference of the three translations from the output of 3dvolreg. The total scan-to-scan movement was then calculated as the Euclidean norm of the translations.

## 2.8. Whole-brain analysis

In addition to the ROI analysis, we also performed a whole-brain group analysis based on spatial normalization to a template MRI (Datta et al., 2012). There are substantial challenges to performing this type of analysis due to the wide variation in size and shape of the dogs' brains. Nevertheless, the following processing pipeline was found to indicate significant caudate activation at the group

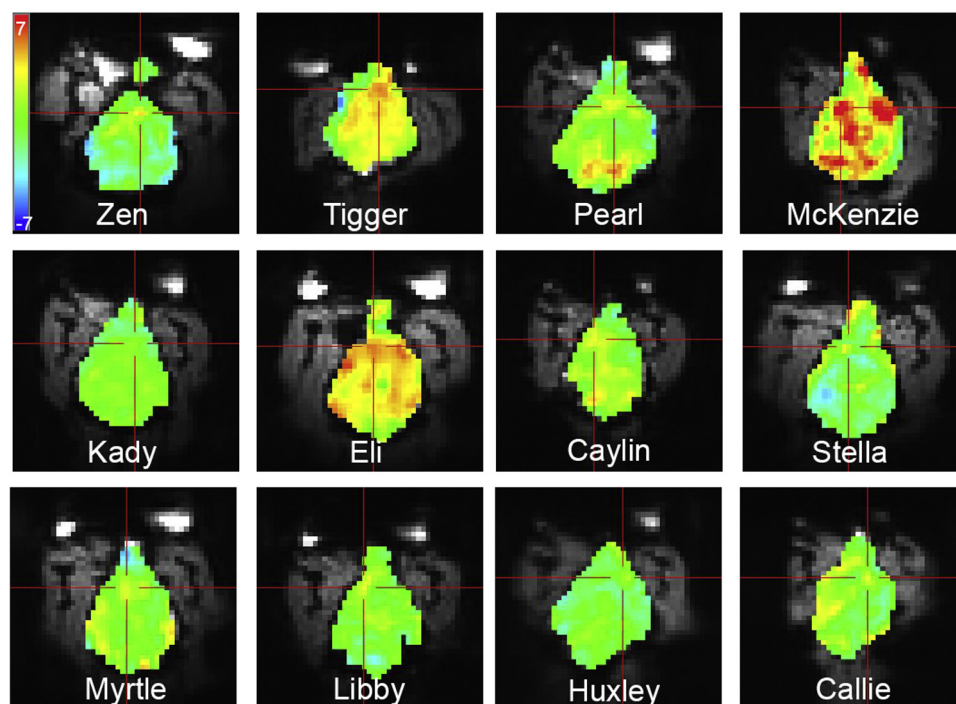


**Fig. 3.** Functional ROI locations for the caudate. Unthresholded whole-brain *t*-maps are displayed for the hand signal indicating imminent food reward (for McKenzie and Eli, the hand signal was too close in time to the reward to separate statistically, so we used the reward contrast for their localizer). The colorbar indicates *t*-values. The area of maximal activation between the anterior extent of the internal capsule and the olfactory bulb was found to closely correspond to the previously identified location of the caudate (Berns et al., 2012, 2013). A spherical ROI of 6 mm radius was placed at this location for extraction of activation within the caudate to the different scents. (For interpretation of the references to color in this figure legend, the reader is referred to the web version of the article.)

level in the dataset from the original reward/no reward experiment (Berns et al., 2013), so we applied the same pipeline to the smell data here.

For each dog, three spatial transformations were computed: (1) rigid-body mean EPI to structural (6 dof); (2) affine structural to template (12 dof); and (3) diffeomorphic structural to template. These transformations were concatenated together and applied to individual contrasts obtained from the statistical model described above. The end result was a contrast image for each dog transformed into template space, allowing the computation of a group level statistic across all dogs. The transformations were computed using the software package, Advanced Normalization Tools (ANTs) (Avants et al., 2011). First, the mean EPI for each dog was calculated from the motion-corrected images after discarding the censored volumes. Using ITK-SNAP (Yushkevich et al., 2006), the brain was then manually extracted by tracing around the edge of the brain in each slice. The brain was also extracted from each dog's structural image. Images were then bias-corrected using the ANTs command N3BiasFieldCorrection. For the EPI to structural registration, we used a rigid-body transformation under the assumption that because the images come from the same dog, no stretching or nonlinear deformation should be necessary. The mutual information (MI) metric was used to determine the best match. For the structural to template transformation, we first resampled the template brain to 1 mm isotropic resolution to provide a target space with cubic voxels (the original template was  $0.42 \text{ mm} \times 0.42 \text{ mm} \times 1 \text{ mm}$ ). We also re-extracted the brain from the template to include the olfactory bulb, which is missing from the published skull-stripped template. Using the MI metric to match the images, we allowed a full affine transformation (12 dof) followed by a diffeomorphic warping using the symmetric normalization (SyN) option.

To apply the transformations to a statistical contrast, the appropriate contrast was extracted from the AFNI BRIK file and converted to NIFTI format. Using the WarpImageMultiTransform command, the three transformation matrices were concatenated together: epi-to-structural (6 dof), structural-to-template (12 dof), structural-to-template (warp field). The end result was a contrast image for each dog in template space. We then used the AFNI command, 3dttest++, to compute a *t*-test across dogs with a null hypothesis that each voxel had a mean of zero. We used all dogs except Zen, who did not have a complete structural image and could not be transformed into the template space.

The following contrasts were examined: (1) main effect of smell (all scents averaged and referenced to the implicit baseline). As above, this was done primarily to verify that olfactory bulb/cortex was activated by the stimuli. (2) Familiar – strange scents, computed as the contrast  $[\text{Hum}_{\text{fam}} + \text{Dog}_{\text{fam}} - \text{Hum}_{\text{str}} - \text{Dog}_{\text{str}}]$ ; and (3) Human–dog scents, computed as the contrast  $[(\text{Hum}_{\text{fam}} + \text{Hum}_{\text{str}})/2 - (\text{Dog}_{\text{fam}} + \text{Dog}_{\text{str}} + \text{self})/3]$ . Because this was still a relatively small sample size, we did not expect highly significant activations. Moreover, correcting for multiple comparisons would result in a highly stringent threshold for significance. We therefore present the unthresholded results to avoid artificially isolating areas of activation and to let readers judge the patterns for themselves (Poldrack et al., 2011). In addition, we used the spatial transformation matrices to map the average location of the functional ROIs onto the template to confirm that the location was in the ventral caudate.

### 3. Results

The olfactory bulb and caudate displayed distinctly different patterns of activation to the five scents (Fig. 4A). The OLF ROI was significantly activated, on average, to all scents [mean = 0.14%,

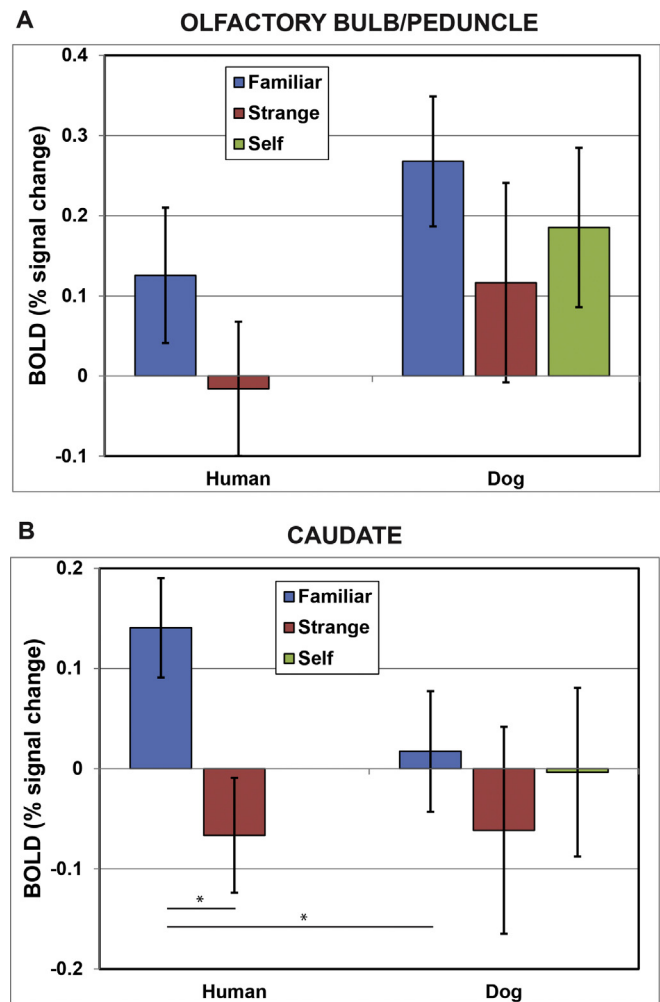


**Fig. 4.** Activation within olfactory bulb and caudate ROIs to different scents. Estimated grand means for each scent are shown  $\pm 1$  s.e. (adjusted for subject wise mean). (A) The olfactory bulb/peduncle was activated, on average, to all of the scents, but ANOVA indicated no significant difference between the scents [ $F(4,13.0) = 1.28$ ,  $p = 0.327$ ]. (B) The caudate, however, showed a significant difference between scents [ $F(4,15.4) = 3.55$ ,  $p = 0.031$ ]. Post hoc contrasts indicated that the scent of a familiar human activated the caudate significantly more than strange human ( $*p = 0.019$ ) and familiar dog ( $*p = 0.043$ ).

s.e. = 0.076%,  $t(11) = 1.79$ , 1-tailed  $p = 0.05$ ]. ANOVA, however, indicated no significant difference between the scents [ $F(4,13.0) = 1.28$ ,  $p = 0.327$ ]. Even when we performed a paired *t*-test on the dog scents versus the human scents, there was still no significant difference [ $t(11) = 1.18$ , 2-tailed  $p = 0.264$ ]. In contrast, while the CD ROI was not active, on average to all scents [mean = 0.01%, s.e. = 0.073%,  $t(11) = 0.14$ , 1-tailed  $p = 0.45$ ], ANOVA indicated a significant difference between the scents [ $F(4,15.4) = 3.55$ ,  $p = 0.031$ ] (Fig. 4B). Post hoc pairwise comparisons indicated that this difference was driven by the scent of the familiar human. Specifically, familiar human was significantly greater than both familiar dog [mean difference = 0.12%, s.e. = 0.055%, 2-tailed  $p = 0.043$ ] and strange human [mean difference = 0.21%, s.e. = 0.079%, 2-tailed  $p = 0.019$ ]. None of the other four scents were significantly different from each other. Interestingly, the service-dogs had a significantly greater overall caudate response to the scents than the other dogs [ $F(1,20.6) = 5.97$ ,  $p = 0.024$ ].

Because subject motion is a potential confounding variable in fMRI experiments due to spin-history effects (Van Dijk et al., 2012; Stoewer et al., 2012), we closely examined the dogs' head movements during scanning. The average scan-to-scan translation

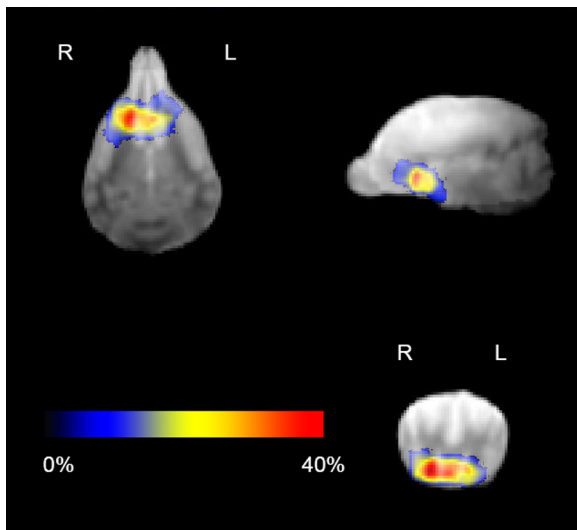


**Fig. 5.** Average location of the functional ROIs. The underlay is the average of the structural images after transformation to the template space. The average location of the ROIs closely overlaid the ventral caudate but was split between the left and right, with peak overlap of approximately 40% on each side.

following the presentation of each scent, before motion correction, was 0.27 mm (s.e. 0.02 mm). Although somewhat greater than the typical movement of humans (Van Dijk et al., 2012), it was less than 1/10th of the voxel size. Importantly, the magnitude of movement was not significantly different in any of the smell conditions [ $F(4,3.2)=0.06$ ,  $p=0.99$ ]. Thus, there was no evidence suggesting that the differences in activation were due to movement that were greater to some scents.

The whole-brain analysis both confirmed the results from the ROI analysis and revealed additional areas of activity. First, the average location of the functional ROI was found to closely overlap the ventral caudate (Fig. 5). Because the side of maximal activity was evenly split between left and right, when averaged together, we observed two areas where there was approximately 40% overlap in the cohort. Second, the average response to all scents showed a pattern consistent with that expected from an olfactory stimulus, with the greatest activation occurring on the border between the olfactory bulb and peduncle (Fig. 6). This location was slightly caudal and superior to where we had placed the ROI, and the

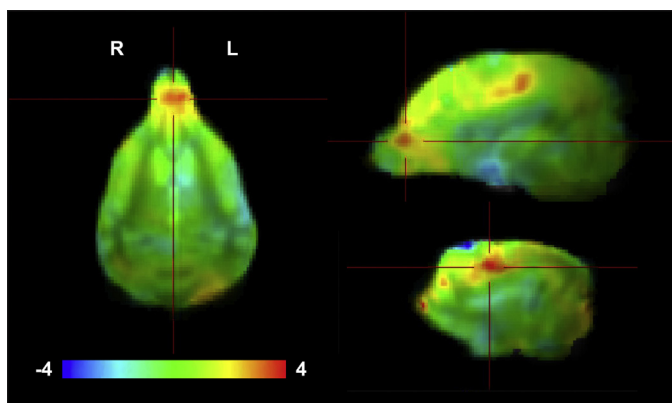


**Fig. 6.** Whole-brain group analysis of response to all scents. A transverse slice (left) and two sagittal slices are shown: midline (upper) and right (lower). Color indicates  $t$ -statistic at each voxel against the null hypothesis of a mean activity of zero referenced to the implicit baseline. The maximal response to all smells was observed in an area on the junction between olfactory peduncle and the olfactory bulb (crosshairs left and upper right). Other areas of potential activation included the left parietal lobe (lower right) and cerebellum.

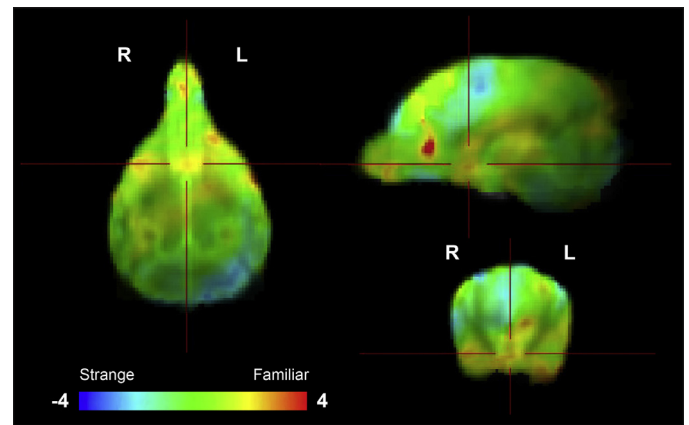


**Fig. 7.** Whole-brain group analysis of differential response to familiar and strange scents. Transverse, sagittal and coronal slices are shown (crosshairs centered on ventral caudate). Color indicates  $t$ -statistic at each voxel against the null hypothesis of equal activity to both familiar and strange scents. Consistent with the ROI analysis, significantly greater activation of the caudate was observed in familiar scents relative to strange scents. Another area of greater activation to familiar scents was noted in the medial frontal lobe just rostral to the genu of the corpus callosum (red). (For interpretation of the references to color in this figure legend, the reader is referred to the web version of the article.)

significance of this activation was notably greater ( $t_{\text{peak}}=3.36$ ,  $p=0.007$ ). Other areas of greater activity included the left parietal lobe and cerebellum. Third, the average differential response to familiar and strange scents (regardless of species), also confirmed the role of the caudate in preferentially responding to familiar scents (Fig. 7). We also noted an area of increased activity in the medial frontal lobe, just anterior to the genu of the corpus callosum. Finally, the average differential response to human and dog scents showed greater activity to dog scents in the same region of the medial frontal lobe, indicating that the response was driven by the scent of the familiar dog (Fig. 8). Conversely, human scents evoked greater activity bilaterally along the sylvian (lateral) fissure.

#### 4. Discussion

The main result is that while the olfactory bulb/peduncle was activated to a similar degree by all the scents, the caudate was activated maximally to the familiar human. Importantly, the scent of

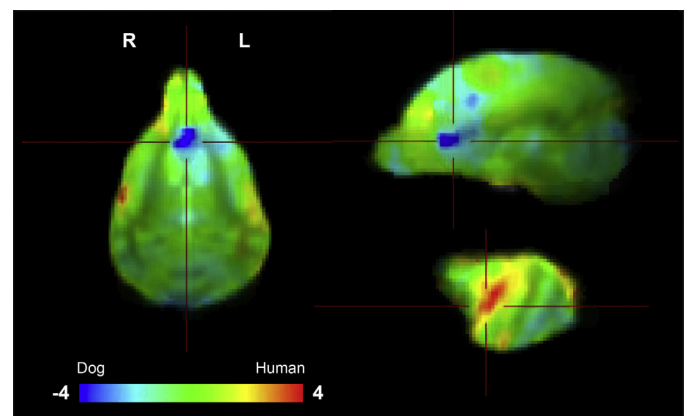


**Fig. 8.** Whole-brain group analysis of differential response to dog and human scents. A transverse slice (left) and two sagittal slices are shown: midline (upper) and right (lower). Color indicates  $t$ -statistic at each voxel against the null hypothesis of equal activity to both dog and human scents. An area of greater activation to dog scents was noted in the medial frontal lobe at the same location as in Fig. 7 for familiar scents. In contrast, greater activity to human scents was observed bilaterally along the sylvian fissure (lower right).



the familiar human was not the handler, meaning that the caudate response differentiated the scent in the absence of the person being present. The caudate activation suggested that not only did the dogs discriminate that scent from the others, they had a positive association with it. This speaks to the power of the dog's sense of smell, and it provides clues about the importance of humans in dogs' lives.

A vast literature on the caudate points to this region's role in positive expectations (Montague and Berns, 2002; Schultz et al., 1997; Knutson et al., 2001), including social rewards (Rilling et al., 2002; Izuma et al., 2008). Indeed, it is tempting to conclude that the caudate response represents something akin to a positive emotional response to the scent of a familiar human (Panksepp, 2004; Bekoff, 2007). Inferring an emotional (or cognitive) state from brain activation, called "reverse inference," has been the subject of much debate in the neuroimaging literature (Poldrack, 2006; Hutzler, 2014; Ariely and Berns, 2010; Machery, 2013). Because most brain regions have multiple functions, it is not usually possible to infer a particular cognitive state from a single activation. The ventral caudate, however, is an exception. More than any other region of the brain, activation here is associated with reward processes to a high probability (c.f. neurosynth.org for meta-analytic probabilities), and this includes both primary rewards like food, social rewards, and, in humans, complex rewards like money, music, and art. It is not clear, however, whether the invocation of a "reward process" is equivalent to a positive emotion. Although positive emotions are usually associated with ventral caudate activity, it is possible that caudate activity may index a motivational state, what Berridge and Robinson termed "wanting" (Berridge and Robinson, 2003) and Panksepp termed "seeking" (Panksepp, 2004). In the most general terms, ventral caudate activity may then be interpreted as a marker to approach the stimulus. This could be out of a desire to consume it or, perhaps, curiosity. In the context of our experiment, it is still significant that only familiar scents, in particular the familiar human, evoked this activity.

Is it possible that the caudate activity represented a conditioned response? There is ample evidence for the caudate's role in appetitive Pavlovian conditioning (O'Doherty et al., 2004; Schultz et al., 1992). But even if the underlying mechanism is Pavlovian, it is still significant because the familiar human (like all the scent donors) was not present during the scanning. Thus, any association would have to be distant in space and time (there was no prospect of immediate reward from the donor human). In that regard, the caudate response resembled that of humans seeing pictures of loved ones who are not physically present (Aron et al., 2005; Noriuchi et al., 2008). However, we cannot rule out the possibility that the familiar humans, at some point in time, had given the dogs food, and that the scent was simply a conditioned stimulus for the dogs. Although possible, we think this unlikely because most of the familiar humans were not the dogs' primary care givers. With the exception of Callie, all of the dogs' handlers were female. The familiar human was either the handler's husband or their child. Most of the handlers reported that they were the ones who fed the dog, and that the husband's or child's interaction with the dog was usually through play.

The whole-brain analysis both confirmed the ROI results and identified additional regions of potential involvement. There are, however, advantages and disadvantages to the ROI and whole-brain approaches. Predefined ROIs have the advantage of statistical efficiency for testing specific hypotheses about the function of a particular brain region. With a small sample size, as we had with the dogs, it was important to be as statistically efficient as possible. With a single ROI, there is no need to correct for multiple comparisons across the whole brain. The disadvantage is that the ROI limits conclusions about brain function to the specific region. ROIs can be defined either anatomically or functionally. An anatomical ROI is usually based on the structural image of the brain, although

it can also be done directly on the functional images if landmarks are clearly visible, as we did previously (Berns et al., 2013). ROI placement can be done individually for each subject, or, if images are transformed to a template space, it can be placed for the entire group. Anatomical ROIs work well when the target is well-defined structurally. In the dog, the olfactory bulb/peduncle is such a structure. The caudate nucleus is also such structure; however, unlike the olfactory peduncle, the left and right caudate are separated by a larger distance, which varies depending on the location within the caudate. As we had previously observed heterogeneity in the activation of the left and right caudate to the hand signal indicating reward, we used a functional ROI to define the location with maximal sensitivity to reward-related signals for each dog. Because the hand-signal was independent of the effects of interest – the scents – we used the hand signal as a "functional localizer" in a manner that was similar to human studies of the visual system (Poldrack, 2007).

The whole-brain analysis overcomes the limitation of focusing on a single region, but it comes at the expense of statistical efficiency. Because the brain is comprised of thousands of voxels in a typical functional image, the likelihood of observing an area of "activation" somewhere in the brain approaches 100%. Most fMRI studies employ some type of correction to control for false positives. This presents a difficult problem for studies with a small number of subjects because the statistical significance with only 12 subjects will not generally survive correction for whole-brain analysis. For this reason, we present the results of the whole-brain analysis as exploratory and as areas for future investigation.

With this caveat, there were a few features of the whole-brain analysis that stood out. First, the location of maximal activation to the scents was located somewhat more caudally and superior to where we located the olfactory ROI. We are not sure why this area was located cortically rather than in the bulb itself. It may be that the hemodynamic response in the bulb is smaller than the cortex. Or, because we used complex, biological stimuli, the cortical response was a downstream, higher level of processing than the molecular primitives that the bulb is thought to process (Jia et al., 2014). This is consistent with a growing body of evidence in the rat that the olfactory cortex binds complex olfactory primitives into a "gestalt" representation (Doucette et al., 2011; Haberly, 2001). Similarly, sniffing may affect the olfactory percept (Kepecs et al., 2006), but the locus of control for sniffing is not known. The cerebellum is a likely candidate (Sobel et al., 1998), and, consistent with this, the whole-brain analysis showed an area of activation in the left cerebellum, but this remains an area for future investigation.

Second, the contrast of familiar vs. strange scents confirmed the ROI results in the caudate (Fig. 7). This is important because it shows convergence between the functionally defined ROIs and the whole-brain analysis, which was anatomically based. Although the functional ROIs did map onto the caudate (Fig. 5), this was split between the left and right. The whole-brain analysis showed that despite the left/right heterogeneity, there was still greater activation to the familiar scents than the strange ones. It is interesting that the functionally defined ROI isolated this effect to the familiar human scent, but the whole-brain analysis suggested that the caudate responded both to familiar humans and familiar dogs. As noted above, caudate activity in this context can generally be regarded as a marker for positive expectation, which may certainly apply to both the humans and dogs in the subjects' households. Because we did not collect data regarding the social relationships of the dogs within the households, it is difficult to interpret whether the familiar-dog activity might be due to expectation of play, social hierarchy, or something else. This, too, may be a fruitful area for future investigation. The specificity of the functional ROI to the familiar human, however, suggests a congruence between different sensory modalities. Because the ROI was defined by the response to a hand signal



from a human, it makes sense that this location should be maximally sensitive to human signals, but it was surprising that this sensitivity extended to other modalities, like smell. Although the caudate appears to be broadly involved in linking motivationally salient signals with action systems in the brain, it is likely that some sort of topography exists in the caudate with different types of signals (e.g. visual, olfactory, human, dog) being located in different locations (Choi et al., 2012; Desrochers and Badre, 2012; Klein and Platt, 2013).

In addition to the caudate, the whole-brain analysis showed an area in the medial frontal cortex that had greater activity to familiar scents. The contrast of human vs. dog scent revealed the same area as more active to dog scents. Thus, the scent of the familiar dog was responsible for this effect in the medial frontal cortex. Very little is known about this region in the dog brain. From the anatomy of other species (e.g. rat and monkey), we know that this region of cortex is a major contributor of input to the ventral caudate (Ongur and Price, 2000). Thus, given the dogs' caudate response to familiar scents, the medial frontal region may represent the source of this input to the caudate. In contrast, the brain regions that were relatively more active to human scents were restricted to the sylvian (lateral) sulcus. This is a large, heterogeneous region of the brain, which encompasses both insular cortex and the bank in the temporal lobe. Insular cortex is known to have diverse functional roles related to internal bodily sensation, including arousal (good and bad), taste, disgust, pain, and empathy (Lamm and Singer, 2010; Kida et al., 2011; Nieuwenhuys, 2012), several of which could play a role in processing biological odors.

Our results raise intriguing questions about the origin of dogs' social flexibility. Was the caudate response the result of selective breeding or social environment? Selective breeding may have created a natural interspecies bond that is stronger than the dogs' innate intraspecies bond. Nine of the 12 dogs were purebred, of which four were from service-dog programs, and the other five were specifically bred to perform in conformation or working shows. Three of the dogs were mixed breeds that were adopted from rescue agencies or shelters. Most likely these dogs emanated from accidental, not purposeful, breeding. Alternatively, the caudate response to familiar humans may be a result of the nurturing environment in which the dogs were raised. All of the dogs were family pets and had been raised by humans since they were puppies. However, because the service dogs were both bred for this job and raised with intense human contact from a young age, this may explain the greater response of their caudates to human scents. Because the same result was obtained in the analysis of the differential response to hand signals indicating the presence or absence of food reward (Berns et al., 2013), the greater caudate responsiveness of the service dogs appears to be a stable trait of the dogs. However, we cannot distinguish the respective roles of heredity from environment in this regard (Udell and Wynne, 2010), or that the difference in service dogs may be due to the small sample size.

But even without interpreting the dog's subjective experience, it is significant that the caudate was more active to the smell of a familiar human than a familiar dog. Because the effect was maximal in the functionally defined ROI, this region of the caudate may represent a convergence of signals from humans, namely a hand signal and a scent. Although these signals came from two different people, the humans lived in the same household as the dog and therefore represented the dog's primary social circle. And while we might expect that dogs should be highly tuned to the smell of conspecifics, it seems that the "reward response" is reserved for their humans. Whether this is based on food, play, innate genetic predisposition, or something else, remains an area for future investigation.

## Acknowledgements

We are grateful to all of the dogs' owners for the time they have devoted to training: Aliza Levenson (Tigger), Melissa Cate (McKenzie), Patricia King (Kady), Darlene Coyne (Zen), Vicki D'Amico (Pearl), Lorraine Backer (Caylin), Lindsay Feters (Eli), Nicole Zitron (Stella), Claire Pearce (Libby), Carol Farren (Myrtle), Donna Kelley (Friday), Melanie Pincus (Huxley), and GB's dog, Callie, for being the first. Thanks to Helen Berns and Lisa LaViers for help on scent duty, and Peter Cook and Erin Hecht for assistance with spatial normalization. Dog photos courtesy: Helen Berns. This work was funded by a grant from the Office of Naval Research (N00014-13-1-0253).

## References

- Alexander, G.E., DeLong, M.R., Strick, P.L., 1986. Parallel organization of functionally segregated circuits linking basal ganglia and cortex. *Annual Review of Neuroscience* 9, 357–381.
- Ariely, D., Berns, G.S., 2010. Neuromarketing: the hope and hype of neuroimaging in business. *Nature Reviews Neuroscience* 11, 284–292.
- Aron, A., Fisher, H., Mashek, D.J., Strong, G., Li, H., Brown, L.L., 2005. Reward, motivation, and emotion systems associated with early-stage intense romantic love. *Journal of Neurophysiology* 94, 327–337.
- Avants, B.B., Tustison, N.J., Song, G., Cook, P.A., Klein, A., Gee, J.C., 2011. A reproducible evaluation of ANTs similarity metric performance in brain image registration. *NeuroImage* 54, 2033–2044.
- Bekoff, M., 2001. Observations of scent-marking and discriminating self from other by a domestic dog (*Canis familiaris*): tales of displaced yellow snow. *Behavioural Processes* 55, 75–79.
- Bekoff, M., 2007. *The Emotional Lives of Animals*. New World Publishers, Novato.
- Berns, G.S., Brooks, A., Spivak, M., 2013. Replicability and heterogeneity of awake unrestrained canine fMRI responses. *PLoS ONE* 8, e81698.
- Berns, G.S., Brooks, A.M., Spivak, M., 2012. Functional MRI in awake unrestrained dogs. *PLoS ONE* 7, e38027.
- Berridge, K.C., Robinson, T.E., 2003. Parsing reward. *Trends in Neuroscience* 26, 507–513.
- Choi, E.Y., Yeo, B.T.T., Buckner, R.L., 2012. The organization of the human striatum estimated by intrinsic functional connectivity. *Journal of Neurophysiology* 108, 2242–2263.
- Darwin, C., 1872. *The Expression of the Emotions in Man and Animals*. John Murray, London.
- Datta, R., Lee, J., Duda, J., Avants, B.B., Vite, C.H., Tseng, B., Gee, J.C., Aguirre, G.D., Aguirre, G.K., 2012. A digital atlas of the dog brain. *PLoS ONE* 7, e52140.
- Daw, N.D., Gershman, S.J., Seymour, B., Dayan, P., Dolan, R.J., 2011. Model-based influences on humans' choices and striatal prediction errors. *Neuron* 69, 1204–1215.
- Desrochers, T.M., Badre, D., 2012. Finding parallels in fronto-striatal organization. *Trends in Cognitive Sciences* 16, 407–408.
- Doucette, W., Gire, D.H., Whitesell, J., Carmean, V., Lucero, M.T., Restrepo, D., 2011. Associative cortex features in the first olfactory brain relay station. *Neuron* 69, 1176–1187.
- Haberly, L.B., 2001. Parallel-distributed processing in olfactory cortex: new insights from morphological and physiological analysis of neuronal circuitry. *Chemical Senses* 26, 551–576.
- Hare, B., Woods, V., 2013. *The Genius of Dogs. How Dogs Are Smarter than You Think*. Dutton, New York.
- Hepper, P.G., 1988. The discrimination of human odour by the dog. *Behavioural Processes* 17, 549–554.
- Hutzler, F., 2014. Reverse inference is not a fallacy per se: cognitive processes can be inferred from functional imaging data. *NeuroImage* 84, 1061–1069.
- Izuma, K., Saito, D.N., Sadato, N., 2008. Processing of social and monetary rewards in the human striatum. *Neuron* 58, 284–294.
- Jia, H., Pustovsky, O.M., Waggoner, P., Beyers, R.J., Schumacher, J., Wildey, C., Barrett, J., Morrison, E., Salibi, N., Denney, T.S., Vodyanov, V.J., Deshpande, G., 2014. Functional MRI of the olfactory system in conscious dogs. *PLoS ONE* 9, e86362.
- Kepecs, A., Uchida, N., Mainen, Z.F., 2006. The sniff as a unit of olfactory processing. *Chemical Senses* 31, 167–179.
- Kida, I., Iguchi, Y., Hoshi, Y., 2011. Blood oxygenation level-dependent functional magnetic resonance imaging of bilateral but asymmetrical responses to gustatory stimulation in the rat insular cortex. *NeuroImage* 56, 1520–1525.
- Klein, J.T., Platt, M.L., 2013. Social information signaling by neurons in primate striatum. *Current Biology* 23, 691–696.
- Knutson, B., Adams, C.M., Fong, G.W., Hommer, D., 2001. Anticipation of increasing monetary reward selectively recruits nucleus accumbens. *Journal of Neuroscience* 21, RC159.
- Koob, G.F., 1992. Drugs of abuse: anatomy, pharmacology and function of reward pathways. *Trends in Pharmacological Science* 13, 177–184.
- Lamm, C., Singer, T., 2010. The role of anterior insular cortex in social emotions. *Brain Structure and Function* 214, 579–591.

- Leigh, E.J., MacKillop, E., Robertson, I.D., Hudson, L.C., 2008. *Clinical anatomy of the canine brain using magnetic resonance imaging*. *Veterinary Radiology & Ultrasound* 49, 113–121.
- Machery, E., 2013. In defense of reverse inference. *British Journal for the Philosophy of Science*, <http://dx.doi.org/10.1093/bjps/axs044>.
- Miklosi, A., 2007. *Dog Behaviour, Evolution, and Cognition*. Oxford University Press, New York.
- Miklosi, A., Topal, J., 2013. What does it take to become 'best friends'? Evolutionary changes in canine social competence. *Trends in Cognitive Sciences* 17, 287–294.
- Montague, P.R., Berns, G.S., 2002. Neural economics and the biological substrates of valuation. *Neuron* 36, 265–284.
- Nieuwenhuys, R., 2012. The insular cortex: a review. *Progress Brain Research* 195, 123–163.
- Noriuchi, M., Kikuchi, Y., Senoo, A., 2008. The functional neuroanatomy of maternal love: mother's response to infant's attachment behaviors. *Biological Psychiatry* 63, 415–423.
- O'Doherty, J., Dayan, P., Schultz, J., Deichmann, R., Friston, K., Dolan, R.J., 2004. Dissociable roles of ventral and dorsal striatum in instrumental conditioning. *Science* 304, 452–454.
- Ongur, D., Price, J.L., 2000. The organization of networks within the orbital and medial prefrontal cortex of rats, monkeys and humans. *Cerebral Cortex* 10, 206–219.
- Palmer, R., Custance, D., 2008. A counterbalanced version of Ainsworth's strange situation procedure reveals secure-base effects in dog–human relationships. *Applied Animal Behaviour Science* 109, 306–319.
- Panksepp, J., 2004. *Affective Neuroscience: The Foundations of Human and Animal Emotions*. Oxford University Press, New York.
- Poldrack, R.A., 2006. Can cognitive processes be inferred from neuroimaging data? *Trends in Cognitive Sciences* 10, 59–63.
- Poldrack, R.A., 2007. Region of interest analysis for fMRI. *Social Cognitive Affective Neuroscience* 2, 67–70.
- Poldrack, R.A., Mumford, J.A., Nichols, T.E., 2011. *Handbook of Functional MRI Data Analysis*. Cambridge University Press, New York.
- Rilling, J.K., Gutman, D.A., Zeh, T.R., Pagnoni, G., Berns, G.S., Kilts, C.D., 2002. A neural basis for social cooperation. *Neuron* 35, 1–20.
- Schoon, G.A.A., de Bruin, J.C., 1994. The ability of dogs to recognize and cross-match human odours. *Forensic Science International* 69, 111–118.
- Schultz, W., Apicella, P., Scarnati, E., Ljungberg, T., 1992. Neuronal activity in monkey ventral striatum related to the expectation of reward. *Journal of Neuroscience* 12, 4595–4610.
- Schultz, W., Dayan, P., Montague, P.R., 1997. A neural substrate of prediction and reward. *Science* 275, 1593–1599.
- Sobel, N., Prabhakaran, V., Hartley, C.A., Desmond, J.E., Zhao, Z., Glover, G.H., Gabrieli, J.D.E., Sullivan, E.V., 1998. Odorant-induced and sniff-induced activation in the cerebellum of the human. *Journal of Neuroscience* 18, 8990–9001.
- Stoewer, S., Goense, J., Keliris, G.A., Bartels, A., Logothetis, N.K., Duncan, J., Sigala, N., 2012. An analysis approach for high-field fMRI data from awake non-human primates. *PLoS ONE* 7, e29697.
- Thesen, A., Steen, J.B., Doving, K.B., 1993. Behavior of dogs during olfactory tracking. *Journal of Experimental Biology* 180, 247–250.
- Topal, J., Miklosi, A., Csanyi, V., Doka, A., 1998. Attachment behavior in dogs (*Canis familiaris*): a new application of Ainsworth's (1969) strange situation test. *Journal of Comparative Psychology* 112, 219–229.
- Udell, M.A.R., Dorey, N.R., Wynne, C.D.L., 2010. What did domestication do to dogs? A new account of dogs' sensitivity to human actions. *Biological Reviews* 85, 327–345.
- Udell, M.A.R., Wynne, C.D.L., 2010. Ontogeny and phylogeny: both are essential to human-sensitive behaviour in the genus *Canis*. *Animal Behaviour* 79, e9–e14.
- Van Dijk, K.R.A., Sabuncu, M.R., Buckner, R.L., 2012. The influence of head motion on intrinsic functional connectivity MRI. *NeuroImage* 59, 431–438.
- Yushkevich, P.A., Piven, J., Hazlett, H.C., Smith, R.G., Ho, S., Gee, J.C., Gerig, G., 2006. User-guided 3D active contour segmentation of anatomical structures: significantly improved efficiency and reliability. *NeuroImage* 31, 1116–1128.